NRC Research Press

ARTICLE

Use of fixed-wing and multi-rotor unmanned aerial vehicles to map dynamic changes in a freshwater marsh[1]

James V. Marcaccio, Chantel E. Markle, and Patricia Chow-Fraser

Abstract: We used a multi-rotor (Phantom 2 Vision+, DJI) and a fixed-wing (eBee, senseFly) unmanned aerial vehicle (UAV) to acquire high-spatial-resolution composite photos of an impounded freshwater marsh during late summer in 2014 and 2015. Dominant type and percent cover of three vegetation classes (submerged aquatic, floating or emergent vegetation) were identified and compared against field data collected in 176 (2 m × 2 m) quadrats during summer 2014. We also compared these data against the most recently available digital aerial true colour, high-resolution photographs provided by the government of Ontario (Southwestern Ontario Orthophotography Project (SWOOP), May 2010), which are free to researchers but taken every 5 years in leaf-off spring conditions. The eBee system produced the most effective data for determining percent cover of floating and emergent vegetation (58% and 64% overall accuracy, respectively). Both the eBee and the Phantom were comparable in their ability to determine dominant habitat types (moderate kappa agreement) and were superior to SWOOP in this respect (poor kappa agreement). UAVs can provide a time-sensitive, flexible, and affordable option to capture dynamic seasonal changes in wetlands, information that ecologists often require to study how species at risk use their habitat.

Keywords: unmanned aerial vehicle, habitat mapping, vegetation identification, wetlands, multi-rotor, fixed-wing.

Résumé : Nous avons utilisé un véhicule aérien sans pilote (UAV) à rotors multiples (Phantom 2 Vision+, DJI) et à voilure fixe (eBee, senseFly) pour obtenir des photographies multiples à haute résolution spatiale d'un marais d'eau douce retenue à la fin de l'été 2014 et 2015. Le type dominant et le pourcentage de couverture de trois classes de végétation (végétation aquatique submergée, flottante ou émergente) ont été identifiés et comparés aux données recueillies sur le terrain en 176 (2 m × 2 m) quadrats au cours de l'été 2014. Nous avons aussi comparé ces données aux plus récentes photographies aériennes numériques à haute résolution en couleur naturelle obtenues du gouvernement de l'Ontario (Southwestern Ontario Orthophotography Project (SWOOP), mai 2010), qui sont disponibles gratuitement aux chercheurs, mais prises tous les cinq ans en conditions printanières sans feuilles. Le système eBee a produit les données les plus efficaces aux fins de la détermination du pourcentage de couverture en végétation flottante et émergente (respectivement, 58 et 64 % d'exactitude générale). Le eBee et le Phantom étaient comparables en matière de leur capacité à déterminer les types d'habitat dominants (concordance kappa modérée) et étaient supérieurs à SWOOP à cet égard (faible concordance kappa). Les UAV peuvent offrir une option flexible et abordable, à délai critique aux fins de saisir les changements saisonniers dynamiques

Received 23 March 2015. Accepted 13 April 2016.

J. V. Marcaccio, C. E. Markle, and P. Chow-Fraser. Department of Biology, McMaster University, 1280 Main St. West, Hamilton, ON L8S 4K1, Canada.
Corresponding author: James V. Marcaccio (email: marcacjv@mcmaster.ca).
[1]This manuscript is part of a special issue based on the International Conference on Unmanned Aerial Vehicles in Geomatics (UAV-g), held from 30 August – 2 September, 2015, in Toronto, Ont., Canada.

des terres humides dont les écologistes ont souvent besoin pour étudier comment les espèces en péril utilisent leur habitat.

Mots-clés : véhicule aérien sans pilote, cartographie de l'habitat, identification de la végétation, terres humides, rotors multiples, voilure fixe.

Introduction

In ecological research, especially in the field of conservation, aerial images are a prerequisite to creating effective management plans for ecosystems and species-at-risk. Without accurate knowledge of what habitat is present and how it is changing, it is difficult to form a management or recovery strategy for endangered species and places. The conventional method of image acquisition, using sensors mounted on planes or satellites, can collect image data for large areas at a time, but can cost tens or hundreds of thousands of dollars depending on the region of interest (Anderson and Gaston 2013). Although these methods can acquire image data for large areas, it can be difficult to use these to obtain data for a specific time period of interest (e.g., year, season or day). For instance, satellites can only obtain photos on days when the image sensor is in line with the study area, and then these photos take time to come to market. Air photos require detailed planning and can be limited by weather and flight regulations. Desired image data may never be obtained for a study site, and consequently researchers and management agencies often have to settle for whatever image data are available. For example, timing of aerial image data collection can limit the ability of investigators to study movement patterns and habitat use of migratory animals (Markle and Chow-Fraser 2014), carry out change-detection analyses (Singh 1989), or monitor the spread of invasive species (Wan et al. 2014).

Recent advancements in technology have opened up a new source for aerial image data: unmanned aerial vehicles (UAVs), commonly referred to as drones. These systems fly without an onboard operator and are controlled remotely from the ground. The proliferation of the "flying camera" market for recreational users has permitted lower prices with consistent improvement in quality of all small-scale UAVs. One of the most important additions to UAVs has been global positioning systems (GPS), with live-feeds of video (first person view, FPV) and base stations that can determine the UAV's location. Equipped with these, a UAV can determine its own location in three-dimensional space and apply this to its image data to allow operators to view the landscape from the UAVs point of view during flight.

Many potential uses of this new technology in the field of ecology are being explored, although not all have yet been attempted or brought to their full realization, especially for time-sensitive research (Rose et al. 2014). Martin et al. (2012) brought this to light, using an artificial study identifying randomly placed and randomly covered tennis balls in the hopes that UAVs can provide a crucial positive application to conservation. Researchers have attempted to quantify the accuracy (e.g., Chabot and Bird 2013; Gómez-Candón et al. 2013) and savings (e.g., Breckenridge et al. 2012) of a UAV-based mapping approach. Breckenridge et al. (2012) found that using a helicopter-style UAV for determining vegetation cover was 45% faster than in-field identification. In addition to faster surveys, they found no difference in vegetation cover interpretation between these techniques (Breckenridge et al. 2012), which could be due to the higher degree of texture seen in UAV image data compared with traditional image data sources like satellites (Laliberte and Rango 2009). An approach with fixed-wing, plane-style UAVs has also been used, which yielded highly accurate images (Koh and Wich 2012; Chabot and Bird 2013). Gómez-Candón et al. (2013) used a quad-copter to produce image data suitable for monitoring agricultural crops, and Wan et al. (2014) monitored growth of invasive species in salt marshes of China. Moreover, they determined that flight paths 30 m above ground only required a few ground-control points to maintain spatial accuracy of these images.

The purpose of our study is to compare the ability of recently available multi-rotor and fixed-wing UAVs to produce image data that permits accurate mapping of wetland vegetation when compared to field-collected vegetation data. We will also compare UAV image data with the most recently available digital aerial photographs provided by a consortium of governments in Ontario (Southwestern Ontario Orthophotography Project (SWOOP) 2010). These orthophotos are true colour and have been acquired during spring (vegetation in leaf-off conditions) at 4 year intervals since 2002. They are commonly used in Ontario research projects because they are provided at no cost to researchers and cover almost all of southwestern Ontario. While many studies have assessed the merits of these technologies with respect to object-based image classification (Laliberte et al. 2011, 2012; Knoth et al. 2013), we present a comparison directly between image data and field data.

Fig. 1. Location of study site: impoundment along the northern shore of Lake Erie.

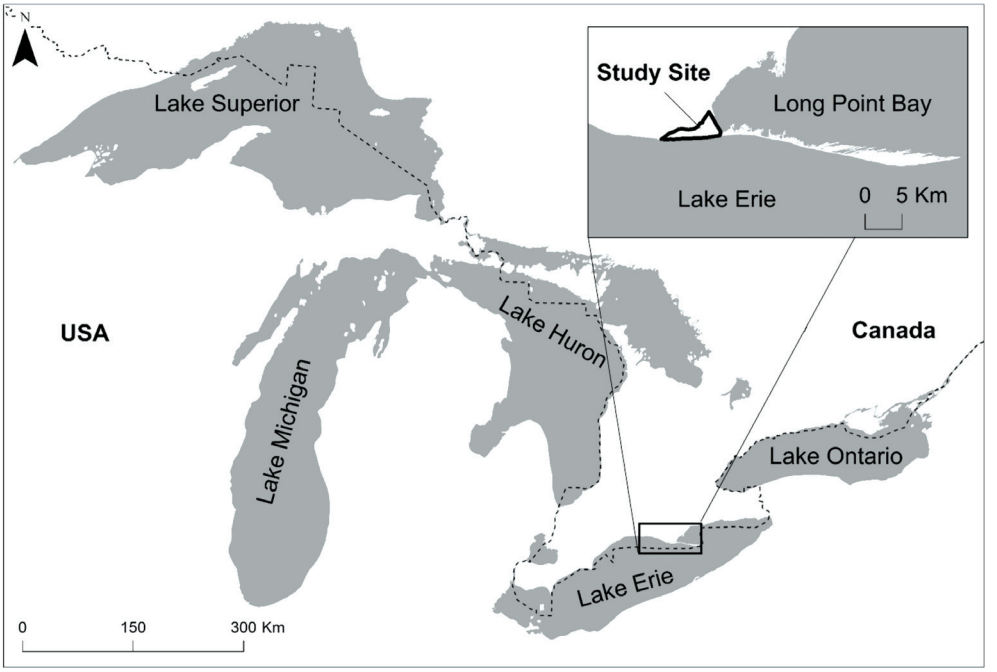

Study site

Our study took place in a 90 ha impounded wetland located within a larger wetland complex along the northern shore of Lake Erie, Ontario (Fig. 1). The owner of the dyked wetland regulates water levels within the impounded area to discourage establishment of invasive emergent species like the non-native *Phragmites australis* spp. *australis* and consequently only a few of these are found within the impoundment. This is in striking contrast to the edge of the impoundment, which is covered with this invasive subtype. Overall, the most common emergent vegetation (EM) in this area is cattail (*Typha* spp.) and swamp loosestrife (*Decodon verticillatus*), along with a variety of floating aquatic vegetation (FL) (e.g., *Nymphaea odorata, Nymphoides peltata*) and submerged aquatic vegetation (SAV) (e.g., *Ultricularia* spp., *Potamogeton* spp.). This diverse and dynamic vegetation community provides habitat for many at-risk turtles, snakes, and birds (Environment Canada 2015).

Materials and methods

Piloted aircraft image acquisition

Image data from piloted aircraft used in this study were obtained from the Southwestern Ontario Orthophotography Project, hereinafter referred to as SWOOP (SWOOP 2010). Various levels of governments provide funds to acquire images (leaf-off conditions) every 5 years for a large portion of southwestern Ontario. We use these image data from piloted aircraft because they are commonly used in Ontario for research and planning purposes, and are similar to aerial image data from piloted aircraft utilized in many countries. We use the most recent image data available, which were captured in spring (April and May) 2010 using a Leica geosystems ADS80 SH82 sensor. These image data have 20 cm resolution with 50 cm horizontal accuracy (see Table 1).

Multi-rotor image acquisition

The multi-rotor UAV used in this study was a DJI Phantom 2 Vision+ (DJI, Nanshan district, Shenzen, China), hereinafter referred to as Phantom, a low-cost unit that is extremely popular among recreational UAV pilots. This was operated with a Samsung Galaxy S3 (running Android 4.3 "Jelly Bean") and the DJI Vision application. The total weight of the system is 1242 g with a DJI 5200 mAh LiPo battery. We kept the remote control at factory settings and flew the UAV with both S1 and S2 levers in the upright position. The S1 lever in this position indicates it is in GPS hold configuration. That is, if the UAV is not given a command it will hold its position regardless of external factors,

Table 1. Comparison of three methods for image data collection.

Parameter	Multi-rotor: DJI Phantom 2 Vision+	Fixed-wing: sensefly eBee	Piloted aircraft: (SWOOP)
Time of data acquisition	User determined This study: Aug 2014	User determined This study: Sept 2015	Spring only every 4–5 years This study: spring 2010
Sensor	DJI FC200 sensor	Canon ELPH 110 HS	Leica geosystems ADS80 SH82 sensor
Spatial resolution (cm)	8	4	20
Cost to researcher (CAD)	1500	30 000	No cost to university researchers under existing data-sharing agreement
Coverage (ha)	65, 16 ha/flight	281, 94 ha/flight	4 500 000, (throughout Southwestern Ontario)
Operator	User manual or automated	User automated	—
Post-processing type and duration	Manual (6–8 h)	Automated (24 h)	—
Lag time	—	—	1 to 1.5 years after image acquisition

Note: SWOOP, Southwestern Ontario Orthophotography Project (spring 2010 edition).

such as wind effects. The S2 lever in the upright position turns off intelligent orientation control. This means that the directional input is always relative to the UAV. For example, pushing the lever forwards will make the drone move forward from its current position, whereas with intelligent orientation control on, pushing the lever forward will move the drone forward with respect to the controller's position.

The UAV was operated with the lens in the 90° position (NADIR) for the duration of the imaging process, and all images were acquired with a DJI FC200 sensor (110° field of view, 1/2.3″ sensor, 14 megapixel, true colour) from a height of 120 m. This flight height was chosen to balance spatial resolution with the amount of flight time required to collect image data for the study area, with a goal of achieving spatial resolution <10 cm and capturing all image data in a single day. We opted to fly the UAV manually rather than use the built-in autopilot system because otherwise we would be limited to a flight distance of 5 km, travelling no further than 500 m from the operator. When autopilot is engaged, the flight speed is 10 m/s, which would only allow for an 8 minute flight plan and result in only two flights per battery. Because this severely limits the area of image data we can collect, we opted for manual operation, which allows us to fly a longer period and thereby capture the majority of the study site. We set the camera on the Phantom to take photos every 3 s (time lapse mode), and set the camera to auto white balance and auto exposure with no exposure compensation. Flight speeds were maintained between 10 and 15 km/h to allow for 60% overlap in post-processing (i.e., image stitching).

We processed the images in Adobe Photoshop Lightroom 5.0 (Adobe Systems Incorporated, San Jose, California, USA) using the lens-correction algorithm provided by DJI for the Vision camera. We cropped images to squares to remove the distortion inherent in the 140° fisheye Vision+ lens. No other modifications were made to the photos. We then used Microsoft ICE (Image Composite Editor; Microsoft Corporation, Redmond, Washington, USA) to stitch together the suite of photos and used the planar motion 1 option to avoid skewing and distortion. This treatment assumes that all of the photos were taken at the same angle, but may have differences in orientation or height above the ground. The mosaic was visually assessed for accuracy stitching before it was used in a GIS.

We manually geo-referenced the stitched image in ArcMap 10.2 (ESRI, Redlands, California, USA) and imported the available SWOOP image data into ArcMap as a base layer. At first, we attempted to use the GPS coordinates directly from the image metadata for geo-referencing, but the accuracy was too low for this purpose. We had to use this method of processing because the GPS information in the geotagged image is not sufficiently accurate to be used in a software such as Pix4D or Photoscan. While the GPS itself has an accuracy of 2.5 m (DJI 2015), this is not stored in the image data. Even though the coordinates are recorded in degrees, minutes, seconds, no decimal places are recorded in the geotagged image, and this results in a grid-like orientation with 20 m accuracy. For example,

if you have two images with different coordinates (43°15′40.19″, 79°55′4.11″ and 43°15′40.45″, 79°55′4.49″), only the rounded coordinates are stored with the image (both geotagged images are now located at 43°15′40.00″, 79°55′4.00″); hence, both images would be placed in the same location even though it is not necessarily the correct location for either image. This is an inherent data reporting issue with Phantom 2 Vision+ models and below, but has been rectified in the Phantom 3 Pro/Advanced models.

In total, we recorded and stitched over 800 images in the Microsoft ICE software. All computations were performed on a Lenovo desktop computer (equipped with Windows 7 64-bit, Intel Core i7-4770 CPU, 12.0 GB RAM, Intel HD Graphics 4600, and a 1 TB hard drive), and the entire process took approximately 6–8 h to create a TIFF file (4.02 GB).

Fixed-wing image acquisition

The fixed-wing UAV used in this study was a senseFly eBee (Parrot, Cheseaux-Lausanne, Switzerland), hereinafter referred to as eBee, with a 96 cm wingspan, 0.25 m^2 wing area, and electric brushless motor. Including the sensor (Canon ELPH 110 HS, true colour) the total weight was 800 g (Styrofoam body). The eBee is powered by a three-cell lithium-polymer battery with each flight lasting approximately 50 min, is hand launched, and cruises at about 27–31 kn, with a landing speed of 2–17 kn for either straight in or circular landing options. The flight plans are pre-programmed in eMotion 2.9 (Parrot, Cheseaux-Lausanne, Switzerland) and the image collection is controlled by autopilot. Onboard, the eBee is equipped with a GPS, barometric pressure sensor, and wind speed sensor. The flight paths were pre-programmed to ensure that complete coverage of the study area is obtained. We conducted all post-processing in PostFlight Terra 3D (Parrot, Cheseaux-Lausanne, Switzerland), which downloads the image data and flight plan from the eBee to create a georeferenced orthomosaic. The eBee is aimed at commercial and industrial users and is the first "compliant UAV" in Canada, meaning government authorities have approved its airworthiness. This also makes flight applications (called Special Flight Operating Certificates) easier and allows for a longer or broader scope of flight areas.

Image data from the eBee were collected on 4 September 2015 during clear-sky conditions and a wind speed of 5 km/h. A total of three flights were completed between 1000 and 1300 h, totalling 30 passes, and taking off and landing occurred in the same spot each flight (Fig. 2). The fixed-wing UAV collected 1319 images that were all pre-processed in PostFlight Terra 3D 3.2 (Fig. 3*b*). All computation was performed on a custom-built desktop (Intel Core i7-4790K CPU, 32GB RAM, EVGA GeForce GT 730 (2GB GDDR5), Samsung 850 Pro 256GB SSD), and the entire process took approximately 24 h to create a TIFF file (6.38 GB).

Field validation data

As part of a separate study on habitat use by several species at risk, we had conducted vegetation surveys of the impounded wetland between 14 July and 14 August 2014. Using a quadrat (2 m × 2 m), we estimated the percent cover of each of the three aquatic vegetation groups (i.e., emergent, submergent, and floating). Separately, each vegetation group was assigned to one of six categories: 0%–10%, 11%–20%, 21%–40%, 41%–60%, 61%–80%, or 81%–100%. If any vegetation was present within the quadrat, we determined the dominant vegetation as that with the highest cover. In total, we collected vegetation information in this way for 176 quadrats. To permit comparisons, we converted the data to three relative percent cover categories: none, <50% cover, or >50% cover. When percent cover was recorded as 41–60%, the result was counted as >50% if only that class existed, or another species of the same class (e.g., *Typha* and grasses are both emergent) was present in another category other than 0%–10% so total cover was over 50%.

To determine dominant vegetation and percent cover from the collected image data, points from the field were plotted in ArcMap 10.2 (ESRI, Redlands, California, USA). A quadrat (2 m × 2 m) was placed around the points to represent area surveyed in the field. These individual points were manually identified by remote sensing of each type of image data (i.e., SWOOP, Phantom, eBee). To calculate dominant vegetation type, the entire quadrat was considered and whichever vegetation (grasses, cattail, submergent, floating) occupied the greatest area was given this class. To calculate percent cover, the relative area that each vegetation type (emergent, submergent, floating) occupied was determined and then directly translated into one of the three classes (i.e., 0, >50%, <50%).

Accuracy analyses

We created 3 × 3 matrices to compare image data (SWOOP, Phantom, eBee) to the field classification separately for percent cover of emergent, submergent, and floating and dominant vegetation type. For each 3 × 3 matrix, we calculated producer and user accuracy in addition to overall

Fig. 2. Flight path taken by the senseFly eBee. Each red dot represents the location of a photo and green lines show the connecting flight path.

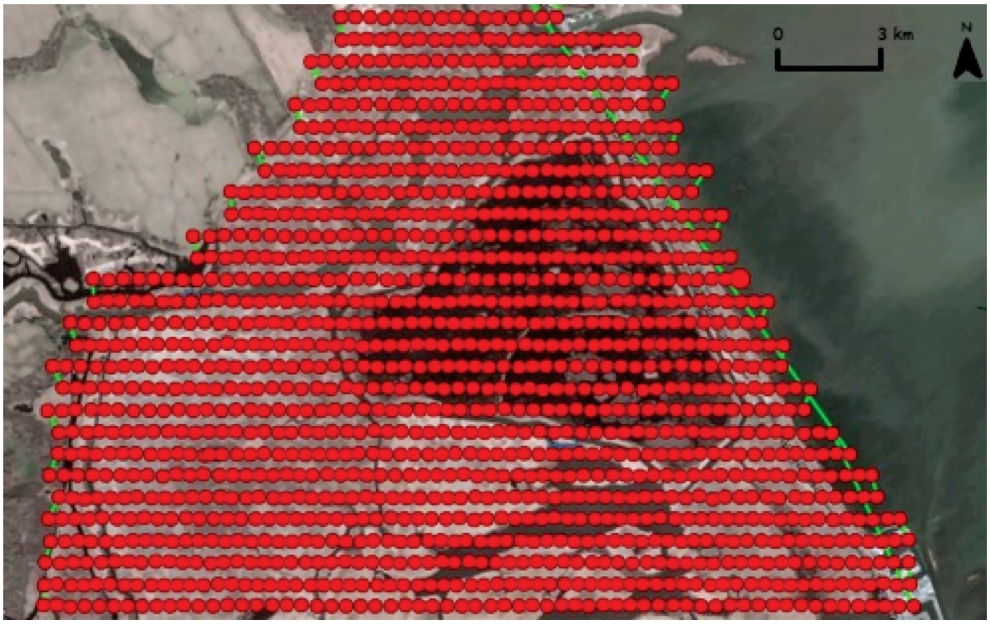

identification accuracy. Producer's accuracy provides an estimate of precision, and is the proportion of plots correctly identified compared to all plots that contain the particular class, whereas user's accuracy, or reliability, is the probability that a plot identified as one class actually belongs to that class. These accuracy measurements were calculated for each class (percent cover: none, up to 50%, over 50%; dominant vegetation: grass, cattail, submerged, and floating or open water). Finally, we provide the kappa estimate to provide a unitless measure of agreement between the image data and field data (Viera and Garrett 2005). It is reported on a scale of no agreement, poor, fair, moderate, good, to very good agreement.

Results

Image data

Using the multi-rotor Phantom, we began flights at 09:00 on 8 August 2014 and ended at 12:00. The UAV was operated from a small grassy patch located on the east side of the impoundment. We completed four flights, 19 passes in total, in favourable weather conditions with wind speeds below 15 km/h and limited cloud cover, with each flight lasting approximately 22 min. Although manual operation was required to achieve desired spatial resolution (<10 cm) and temporal resolution (all image data collected on a single day), image data for a section of the wetland were missing (Fig. 3*a*). We were unable to obtain comprehensive coverage of the entire dyked impoundment because after changing the batteries and re-launching the UAV, it was difficult to ascertain where the previous flight path had stopped, and this led to missing data in the final mosaic. The UAV itself does not record its flight path and therefore we were unable to download this to view previously flown areas. This is a trade-off between manual operation and automatic operation for this multi-rotor platform. While manual operation permits longer flying times and longer flying distances to maximize area of capture, it can result in sections of missing data, as was the case in our study.

The total root mean square error (of the georectification process) for the completed image from the multi-rotor UAV was below 5.0 m, and visual observations confirmed a good fit of the UAV-acquired image to the SWOOP dataset. The image had a resolution of 8.0 cm/pixel as defined in ArcGIS (Table 1). The final image data from the fixed-wing UAV had a spatial resolution of 4 cm/pixel as defined in ArcGIS (Table 1). In addition, a digital elevation model was created by PostFlight Terra 3D in areas where sufficient image overlap existed, although this data was not used in this study.

Fig. 3. Comparison of (*a*) mosaic image acquired with multi-rotor UAV; (*b*) mosaic image acquired with the fixed-wing UAV; and (*c*) SWOOP image. The red line indicates the boundary of the impoundment and survey site.

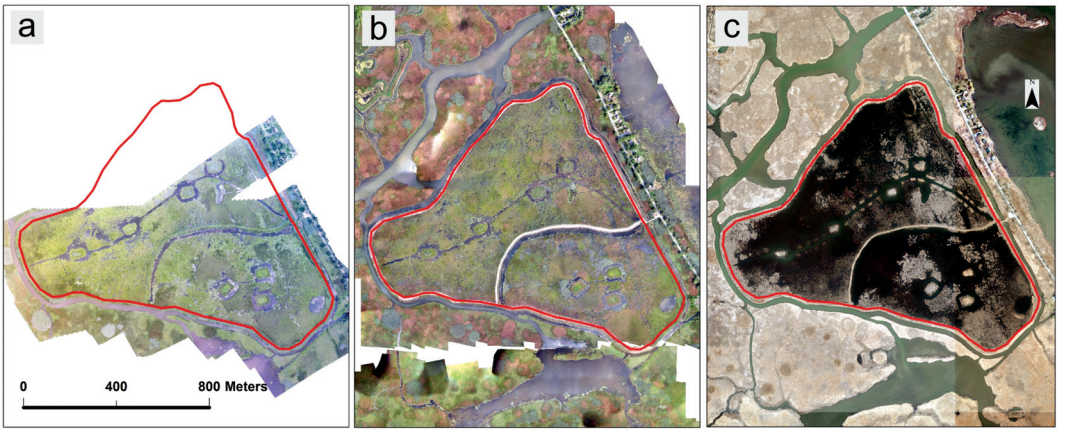

Accuracy analyses

Both the Phantom and eBee were comparable when used to identify dominant vegetation, with an accuracy of 62%–65% (Table 2). Both image data sources were in moderate agreement with field data, with the lowest identification accuracies for floating vegetation. The Phantom and eBee data were both sufficient to identify grass and cattail as the dominant habitat class with accuracies ranging from 60% to 80% (Table 2). In comparison, the SWOOP image data were in poor agreement with the field data because of the difference in timing between the field survey and image data capture and had an overall identification accuracy of 35% (Fig. 3*c* and Table 2). This source of image data failed to accurately identify any of the dominant vegetation classes.

Identification accuracies varied among image data collection methods when used to determine the percent cover of emergent, submerged, and floating vegetation. When determining percent cover of emergent vegetation, the eBee produced a 64% accurate identification and was a fair match with the field data (Table 3). The majority of the confusion occurred when identifying an area with less than 50% cover. The Phantom had a similar problem with this class, which resulted in a slightly lower overall accuracy of 55%, but was still a fair match to the field data (Table 3). The SWOOP image data were only able to identify percent cover of emergent vegetation with an accuracy of 39%, and had the poorest agreement with ground truth data of the three methods evaluated (Table 3).

All methods had high overall accuracy when used to identify submerged vegetation; however, we must interpret these cautiously because none of the field plots had over 50% submergent vegetation cover, and this meant that only two classes (no submergent vegetation and less than 50% submergent vegetation) were identified. Between these two remaining classes, user accuracy was quite low for the below 50% cover class (Phantom, 0.52; SWOOP, 0; eBee, 0.44; Table 3). This indicates that image data were very good at interpreting locations with no submergent vegetation, but not as good at identifying the amount of cover. For example, SWOOP was unable to identify the cover of submerged vegetation, had 0% reliability and 0% precision, and consequently no agreement with the field data (Table 3). In comparison, the Phantom and eBee methods had moderate to fair agreement, respectively, with the field data (Table 3).

The identification accuracy of floating vegetation cover ranged from 18% for SWOOP, 35% for the Phantom and 58% for the eBee (Table 3). The SWOOP image data were completely insufficient to identify floating vegetation, and yielded 0% producer and user accuracy for both cover classes (Table 3). Both the Phantom and SWOOP image data had poor agreement with field data, whereas the eBee was in fair agreement (Table 3).

Discussion

Use of a multi-rotor or fixed-wing UAV is of particular interest for mapping coastal wetlands because these ecosystems are dynamic, and experience seasonal and interannual fluctuations in water levels that greatly influence the vegetation community (Midwood and Chow-Fraser 2012). As a result, during the growing season, coastal wetlands can often appear as large open bodies of water in

Table 2. Accuracy values calculated for each method when image data are compared with field data for respective types of dominant vegetation.

		Class					
Method type	Accuracy	Grass	Cattail	Submerged	Floating	Kappa assessment	Overall accuracy
Phantom	Producer	0.693	0.565	0.910	0.465	Moderate	62%
	User	0.658	0.667	0.910	0.435		
eBee	Producer	0.813	0.630	0.910	0.302	Moderate	65%
	User	0.656	0.690	1.000	0.433		
SWOOP	Producer	0.750	0.475	0.002	0	Poor	35%
	User	0.300	0.463	0.334	n/a		

Table 3. Accuracy values calculated for each method when image data are compared to field data. n/a indicates that no field plots exist for this class.

			Class (percent cover)				
Vegetation type	Method	Accuracy type	None	Up to 50% cover	Over 50% cover	Kappa assessment	Overall accuracy
Emergent	Phantom	Producer	0.733	0.226	0.8	Fair	55%
		User	0.379	0.459	0.623		
	eBee	Producer	0.666	0.387	0.869	Fair	64%
		User	0.625	0.690	0.624		
	SWOOP	Producer	0.666	0.480	0.259	Poor	39%
		User	0.172	0.444	0.611		
Submerged	Phantom	Producer	0.786	0.833	n/a	Moderate	83%
		User	0.983	0.521	n/a		
	eBee	Producer	0.765	0.667	n/a	Fair	75%
		User	0.941	0.444	n/a		
	SWOOP	Producer	0.979	0	n/a	No agreement	81%
		User	0.826	0	n/a		
Floating	Phantom	Producer	0.677	0.316	0.148	Poor	35%
		User	0.236	0.649	0.138		
	eBee	Producer	0.581	0.675	0.148	Fair	58%
		User	0.327	0.693	0.667		
	SWOOP	Producer	1.000	0	0	Poor	18%
		User	0.177	0	0		

the spring, and undergo seasonal succession to a completely vegetated habitat towards late summer (see Fig. 4). This characteristic is one of the main reasons that coastal wetlands can support high biodiversity, and provide unique, sometimes critical, habitat for many species at risk. This dynamic nature of coastal marshes means that a single image acquired at the beginning of the season (such as SWOOP) is inappropriate for mapping habitat that is used by species later in the season. This situation is challenging for most researchers, who lack funds to acquire their own image data at the most appropriate time of the season, and who must use publically available orthophotoimagery. This may also explain the lightning speed at which UAVs have been adopted by wetland ecologists over the past year.

We found that the eBee system produced the most effective data for determining percent cover of floating and emergent vegetation compared to the SWOOP and Phantom image data. For submergent vegetation identification, all methods had high accuracy (75%–83%), although this is likely inflated because plots with no submergent vegetation are almost impossible to identify incorrectly. Logically, when determining percent cover of emergent and floating vegetation, image data in the summer season with high spatial accuracy is best. But, if the goal is to determine where submergent vegetation will or will not colonize, publically available spring images were able to determine this just as well as the UAV-acquired image data. For both UAV platforms, percent cover of vegetation was identified

Fig. 4. Comparison of (*a*) mosaic image acquired with multi-rotor UAV; (*b*) mosaic image acquired with the fixed-wing UAV; and (*c*) SWOOP image. Details associated with the floating and submersed aquatic vegetation in (*a*) and (*b*) are absent in (*c*).

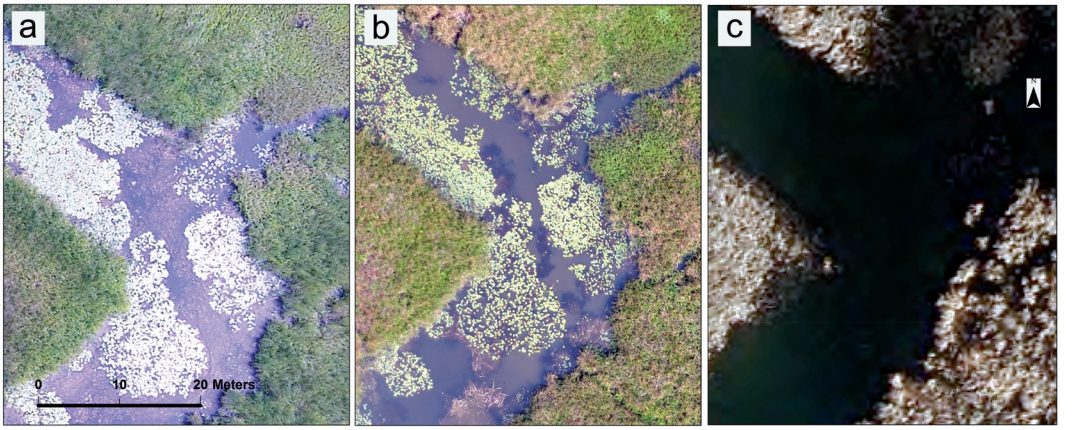

with 55%–83% accuracy (eBee 58%–75%; Phantom 55%–83%) and dominant vegetation type with 62%–65% accuracy. This large range underscores how image data can vary in a dynamic ecosystem. Even though the two UAV images were acquired at roughly the same time of year over two consecutive years, there were marked differences between them (Figs. 3 and 4).

Both multi-rotor and fixed-wing platforms can allow researchers to acquire aerial images of their study sites at a time in the year that is most relevant to their study objectives. When compared to aerial image data acquired by mounting cameras on an airplane, the Phantom and eBee were much more cost-effective. For example, for a wetland of the size in this study (approximately 90 ha), it would have taken two researchers 6–8 days to complete all of the field work to generate a habitat map. By comparison, acquiring images with the UAV only took 6–24 h (Table 1). While up to $5000 CAD would be required to map even a small area by plane, the Phantom, with extra batteries, case, and a tablet or phone for viewing, cost less than $3000 CAD. If the desired mapping area is a few hundred hectares in size, the eBee would be more effective, but involves a higher cost of $30 000 CAD. The benefit in both cases, however, is that these are one-time costs, and maintenance and operation costs are relatively low (Phantom spare propellers, the most frequently broken part, can be obtained for $5 CAD each).

While the Phantom can be useful for mapping small areas (<100 ha), restrictions in data reporting (coordinates, flight plans) capabilities limited its functionality. For instance, we attempted automatic geo-rectification to reduce the time required, but the GPS accuracy on the Phantom was too low for this purpose. Recently, Pix4D released an Android application to improve mapping and geo-rectification called Pix4DMapper (Pix4D, Xuhui District, Shanghai, China), but it requires the use of their own software and can only map relatively small areas at one time (maximum 200 m by 120 m; 2.4 ha) compared to manual flight (with 60% overlap, approximately 20 ha). In total, using autopilot would have garnered less than 20% of the area obtained during our three flights (65 ha; Table 1). This being said, the Phantom Vision 3 Series does provide the GPS coordinate accuracy required to overcome these challenges.

Even though we found SWOOP to be inferior to the UAV-acquired image data, it is freely available for research and ideal for other research applications (e.g., planning and agriculture). Limitations discussed in this study are more of a reflection of the image data being collected in the spring, long before floating and submerged vegetation are fully established (Fig. 4). Overall, our comparison highlights how technological advances can improve our ability to map dynamic systems like coastal wetlands.

Conclusion

The flexibility of UAVs for research and monitoring will revolutionize the way we address and solve ecological problems, especially in dynamic coastal wetlands. The resulting high spatial and temporal resolution image data will permit investigators to ask questions previously limited by traditional imaging technologies. We confirmed that the UAV-acquired images could be used to estimate

the percent cover of three broad classes of wetland vegetation (submerged aquatic vegetation, floating aquatic vegetation, and emergent vegetation) with fair to moderate agreement with field data. To achieve a more exact picture of vegetation communities, we recommend using a UAV platform to acquire image data precisely when desired. By comparison, image data from SWOOP were insufficient to determine dominant vegetation type and percent cover for emergent and floating aquatic vegetation, which comprise a large portion of the study site in the summer season.

As demonstrated, the timing of aerial image acquisition can limit the extent of our research. Seasonal image data can greatly improve our mapping of dynamic wetland ecosystems and allow managers to develop more effective recovery strategies for species-at-risk. Acquiring images multiple times during a single season would have been prohibitively expensive with traditional large plane or satellite platforms, but with low-cost UAVs, this is no longer an obstacle. Researchers no longer need to use commercially available image data that are out-of-date or taken during the wrong season, and instead, learn to create their own. We hope that this study will affirm the use of UAVs in ecological coastal wetland research while encouraging more research into this emerging and inexpensive remote sensing platform.

Acknowledgements

We would like to thank Julia Rutledge and Rebecca Graves for their assistance in collecting the field data for this project. We also acknowledge CGS-D Scholarship to CEM from the Natural Sciences and Engineering Research Council of Canada, the Species at Risk Stewardship Fund to PC-F from the Ontario Ministry of Natural Resources, Habitat Stewardship Program from Environment Canada, and a research grant from the Sierra Club Canada Foundation. This work was completed with a Special Flight Operations Certificate (ATS-15-16-00017451).

References

Anderson, K., and Gaston, K.J. 2013. Lightweight unmanned aerial vehicles will revolutionize spatial ecology. Front. Ecol. Environ. **11**(3): 138–146. doi: 10.1890/120150.

Breckenridge, R.P., Dakins, M., Bunting, S., Harbour, J.L., and Lee, R.D. 2012. Using unmanned helicopters to assess vegetation cover in Sagebrush Steppe ecosystems. Range. Ecol. Manag. **65**(4): 362–370. doi: 10.2111/REM-D-10-00031.1.

Chabot, D., and Bird, D.M. 2013. Small unmanned aircraft: Precise and convenient new tools for surveying wetlands. J. Unmanned Veh. Syst. **1**(1): 15–24. doi: 10.1139/juvs-2013-0014.

DJI. 2015. *Naza – M V2 Quick Start Guide* (V. 1.28). Available from http://dl.djicdn.com/downloads/nazam-v2/en/NAZA-M_Quick_Start_Guide_v1.28_en.pdf. [accessed 14 January 2016].

Environment Canada. 2015. Big creek national wildlife area. Available from www.ec.gc.ca. [accessed 1 November 2015].

Gómez-Candón, D., De Castro, A.I., and López-Granados, F. 2013. Assessing the accuracy of mosaics from unmanned aerial vehicle (UAV) imagery for precision agriculture purposes in wheat. Precis. Agric. **15**(1): 44–56. doi: 10.1007/s11119-013-9335-4.

Knoth, C., Klein, B., Prinz, T., and Kleinebecker, T. 2013. Unmanned aerial vehicles as innovative remote sensing platforms for high-resolution infrared imagery to support restoration monitoring in cut-over bogs. Appl. Veg. Sci. **16**(3): 509–517. doi: 10.1111/avsc.12024.

Koh, L.P., and Wich, S.A. 2012. Dawn of drone ecology: Low-cost autonomous aerial vehicles for conservation. Tropical Conservation Science. **5**(2): 121–132

Laliberte, A.S., Browning, D.M., and Rango, A. 2012. A comparison of three feature selection methods for object-based classification of sub-decimeter resolution UltraCam-L imagery. Int. J. Appl. Earth Obs. **15**: 70–78. doi: 10.1016/j.jag.2011.05.011.

Laliberte, A.S., Goforth, M.A., Steele, C.M., and Rango, A. 2011. Multispectral remote sensing from unmanned aircraft: Image processing workflows and applications for rangeland environments. Remote Sens. **3**(12): 2529–2551. doi: 10.3390/rs3112529.

Laliberte, A.S., and Rango, A. 2009. Texture and scale in object-based analysis of subdecimeter resolution unmanned aerial vehicle (UAV) imagery. IEEE Transcations on Geoscience and Remote Sensing. **47**(3): 761–770. doi: 10.1109/TGRS.2008.2009355.

Markle, C.E., and Chow-Fraser, P. 2014. Habitat selection by the Blanding's turtle (*Emydoidea blandingii*) on a protected island in Georgian Bay, Lake Huron. Chelonian Conserv. Bi. **13**: 216–226. doi: 10.2744/CCB-1075.1.

Martin, J., Edwards, H.H., Burgess, M.A, Percival, H.F., Fagan, D.E., Gardner, B.E., Ortega-Ortiz, J.G., Ifju, P.G., Evers, B.S., and Rambo, T.J. 2012. Estimating distribution of hidden objects with drones: From tennis balls to manatees. PLoS One. **7**(6): e38882, doi: 10.1371/journal.pone.0038882.

Midwood, J.D., and Chow-Fraser, P. 2012. Changes in aquatic vegetation and fish communities following 5 years of sustained low water levels in coastal marshes of eastern Georgian Bay, Lake Huron. Glob. Change Biol. **18**: 93–105. doi: 10.1111/j.1365-2486.2011.02558.x.

Rose, R.A., Byler, D., Eastman, J.R., Fleishman, E., Geller, G., Goetz, S., Guild, L., Hamilton, H., Hansen, M., Headley, R., Jewson, J., Horning, N., Kaplin, B.A., Laporte, N., Leidner, A., Leimgruber, P., Morisette, J., Musinsky, J., Pintea, L., Prados, A., Radeloff, V. C., Rowen, M., Saatchi, S., Schill, S., Tabor, K., Turner, W., Vodacek, A., Vogelmann, J., Wegmann, M., Wilkie, D., and Wilson, C. 2014. Ten ways remote sensing can contribute to conservation. Conserv. biol. **29**(2): 350–359. doi: 10.1111/cobi.12397.

Singh, A. 1989. Review article digital change detection techniques using remotely-sensed data. Int. J. Remote Sens. **10**(6): 989–1003. doi: 10.1080/01431168908903939.

SWOOP (Southwestern Ontario Orthophotography Project). 2010. Ontario Ministry of Natural Resources and Forestry, Hamilton, Ont. Available from Scholars GeoPortal http://geo2.scholarsportal.info/. [accessed 1 November 2015].

Viera, A.J., and Garrett, J.M. 2005. Understanding interobserver agreement: The kappa statistic. Fam. Med. **37**: 360–363

Wan, H., Wang, Q., Jiang, D., Fu, J., Yang, Y., and Liu, X. 2014. Monitoring the invasion of *Spartina alterniflora* using very high resolution unmanned aerial vehicle imagery in Beihai, Guangxi (China). Sci. World J. **2014**: 1–7. doi: 10.1155/2014/638296.